JOURNAL OF AIRCRAFT
Vol. 40, No. 3, May–June 2003

Modeling the Mutual Distortions of Interacting Helicopter and Aircraft Wakes

G. R. Whitehouse* and R. E. Brown†
Imperial College, London, England SW7 2BY, United Kingdom

Flight procedures that will decrease the following distance between successive aircraft have been considered as a means of alleviating pressures on airport capacity while still conforming to conventional air traffic management rules. A major limitation to the implementation of such procedures is perceived to be an associated increase in the possible severity of encounters with the wakes of nearby aircraft. Modeling efforts have focused on quantifying such interactions in terms of structural loading or degradation in handling and have established that helicopters respond in a fundamentally different way than fixed-wing aircraft to encounters with wake vortices. This paper suggests that, particularly at the low forward speeds typical of terminal phase operations, the mutually induced distortion of the helicopter's own wake and the wake of the interacting aircraft strongly influences the aerodynamics of the helicopter rotor. Results from numerical simulations suggest that neglecting this aspect of the interaction, as has commonly been done in the past, can indeed be valid at high helicopter forward speeds, but can lead to significant misrepresentation of the severity of wake encounters under terminal flight conditions.

Nomenclature

A = rotor disc area πR^2
a = aerofoil lift-curve slope
C_L = blade local lift coefficient
C_T = rotor thrust, scaled by $\rho A\,(\Omega R)^2$
C_T^* = rotor thrust under trimmed conditions
c = blade chord length, scaled by R
I_β = blade flapping inertia, scaled by $\rho A R^3$
M = disc-weighted moment of vortex velocity
N = number of rotor blades
R = rotor radius
r = vortex or rotor radial coordinate, scaled by R
r_c = vortex core radius, scaled by R
S = vorticity source, scaled by $\Omega^2 R^2$
v = flow velocity, scaled by ΩR
v_c = tangential velocity at outer edge of vortex core, scaled by ΩR
v_i = induced velocity normal to rotor disc, scaled by ΩR
α = blade local angle of attack
β = blade flapping angle
β_0 = rotor coning angle
β_{1c} = rotor longitudinal tilt angle
β_{1s} = rotor lateral tilt angle
γ_β = rotor Lock number $ac/\pi I_\beta$
θ = blade local feathering angle
μ = rotor advance ratio (forward speed scaled by ΩR)
σ = rotor solidity Nc/π
ψ = blade azimuth
Ω = rotor rotational speed $\mathrm{d}\psi/\mathrm{d}t$
ω = natural frequency of blade flapping, scaled by Ω
ω = flow vorticity, scaled by ΩR^2

Introduction

AN issue of current concern to transport planners is the positioning of helicopter final approach and takeoff areas for the simultaneous operation of rotary and fixed-wing aircraft from airfields. Pressures exist to decrease the separation between successive fixed-wing arrivals or departures, to make maximal use of available ground at airfields, and indeed to promote the use of helicopters in increasing airport capacity.[1]

In the fixed-wing community a major and legitimate practical concern is that an encounter with a concentrated wake vortex, left lying parallel to the aircraft's flight path on the approach to, or departure from, a runway by the earlier passage of another aircraft might be sufficiently strong to induce a roll rate on the airframe, which is larger than can be overcome by full aileron deflection.

Concerns in the helicopter world mirror those of the fixed-wing community because helicopters are presently required to fit into established fixed-wing flight patterns during joint operations from airfields. Helicopters have a fundamentally different response to vortex encounters compared to fixed-wing aircraft, however, and a long-standing debate has been whether their behavior is more or less severe, as gauged by some appropriate measure, than in the fixed-wing case.[2] The response of a helicopter is complicated by aerodynamic cross coupling between the pitch and roll response of the rotor and the filtering of aerodynamic loads that is provided by the various possible methods of attaching the rotor blades to their hubs. On a conventionally configured helicopter at least, these effects tend to dominate the fixed-wing aircraft-like behavior of the fuselage.[2]

Our understanding of the aeromechanical behaviour of helicopters during wake encounters is based almost exclusively upon a series of papers detailing various numerical simulations of idealized helicopters interacting with representative model wake structures. These simulations have been used to quantify the loading changes, rotor flapping response or flight-path deviations that might arise during typical wake encounters. More recent approaches[3,4] have attempted to evaluate the outputs of simulations in terms of quantitative measures of helicopter handling qualities such as those laid out in the ADS-33 airworthiness standard. Validation of these numerical studies has always been hampered, however, by the relatively small and somewhat dated body of supporting experimental data. In the absence of suitable validation data, the issue of modelling fidelity remains largely unresolved.

In this paper we explore one aspect of this issue by examining the validity of the so-called "frozen-vortex" assumption adopted in most previous numerical studies of wake interactions. This assumption holds that the mutually induced distortion of the helicopter's own wake and the wake of the interacting aircraft contributes insignificantly to the aerodynamic loading on the helicopter's rotor and hence to the subsequent dynamics of the helicopter. Although this

Received 26 March 2002; revision received 19 October 2002; accepted for publication 13 February 2003.

*Postgraduate Research Assistant, Department of Aeronautics. Student Member AIAA.
†Lecturer, Department of Aeronautics.

assumption is plausible when the helicopter is flying at high speed (so that these distortions reach appreciable magnitudes only some distance behind the helicopter rotor), the validity of this approach is more doubtful at low helicopter forward speeds. The concern is that extrapolation of the results of previous simulations obtained using the frozen-vortex assumption might not be appropriate if we want to understand helicopter behavior during wake encounters at low forward speeds, or, in other words, under conditions representative of terminal flight operations.

Frozen Vortex Assumption

The aerodynamic model within any numerical simulation of a wake-vortex interaction has three basic components. The rotor aerodynamic model (A), in which the aerodynamic environment of the rotor is translated into rotor loads, requires inputs from a model of the helicopter wake (W) and a model for the interacting vortex (V). The frozen-vortex assumption is best defined in terms of the interactions that can take place between these three models. The response of each component (A, W, or V) to inputs from each other component of the aerodynamic model can be classified as static (no dependence on the inputs to the model), quasistatic (algebraic dependence on inputs), or dynamic (integrodifferential dependence). The following classification provides a useful and compact means of defining a hierarchy, in terms of modelling fidelity, of all possible aerodynamic simulations of vortex encounters. The strongest (level 3) implementations of the frozen-vortex assumption constrain both the wake model and the vortex model to remain static throughout the course of the simulation. Intermediate (level 2) implementations of the assumption allow the wake model to respond quasistatically or dynamically to the rotor loading, whereas the weakest (level 1) implementations of the assumption allow the wake model to respond directly to both the presence of the vortex and to the rotor loading. Complete elimination of the frozen-vortex assumption (yielding a level 0 simulation) requires the interacting vortex, in addition, to respond dynamically to its self-induced velocity field as well as to the presence of the rotor wake.

Previous Work

In their 1976 experimental studies flying a Bell UH-1H parallel to the wake of a Douglas C-54 Skymaster, Dunham et al.[5] and Mantay et al.[6,7] provided the first objective assessment of the severity of an encounter between a helicopter and the wake of a large transport aircraft. They concluded that the maximum load factor of 1.8 g experienced during an interaction with the C-54 wake (at least for following distances greater than 0.42 n miles) was well within the helicopter's safe operating limits. This single set of experiments precipitated a small body of numerical simulations that largely supported its conclusions. This led to a decline in interest in the field in the late 1980s. These studies were largely concerned, however, with the response of the helicopter to wake encounters in free air. It was not until the more recent studies by Padfield and Turner,[3,4] where the severity of a wake encounter was judged in terms of its impact on aircraft handling qualities, that the effect of the operating environment of the helicopter could be acknowledged in any objective manner. Their observation that loading perturbations of the magnitude observed in the earlier experimental and computational works could pose significant piloting problems under terminal flight conditions has sparked a resurgence of interest in the field.

The earliest numerical study appears to have been conducted by Dreier[8] in 1977. He modeled the helicopter as an isolated, articulated rotor with linear blade aerodynamics (up to the stall) and rigid blades. A uniform inflow distribution on the rotor was determined from trim conditions then held constant throughout the simulation. Interaction with another aircraft's wake was modeled by superimposing on the rotor a velocity field designed to represent a vortex with McCormick et al.'s[9] logarithmic velocity distribution lying parallel to the rotor's flight path. This velocity field was also held invariant throughout the simulated interaction, resulting in a level 3 aerodynamic simulation. Dreier's study succeeded in reproducing, both in magnitude and trend, the fundamental flapping and loading response of the helicopter rotor expected from a simple blade-element based theory. This was despite some anomalies that he attributed to the poststall behavior of his blade aerodynamic model.

Saito and coauthors[10–12] provided a significant advance in modeling fidelity by using Azuma's[13] local momentum theory to allow quasistatic coupling between the local rotor aerodynamic loading and the induced flow through the rotor. The wake of the interacting aircraft was modeled by a time-invariant two-dimensional velocity field, through which the helicopter could be flown, yielding a level 2 aerodynamic simulation of the interaction. The resultant loads on the rotor hub were coupled into a six-degree-of-freedom dynamic model for the helicopter fuselage, allowing the effects of a wake encounter on the helicopter's flight path and rigid-body rotation rates to be modeled. These works succeeded in exposing major differences in the behavior of fixed-wing aircraft and helicopters and illustrated the basic differences in behavior between helicopters having rotors with articulated or hingeless hub designs.

A further advance in level 2 aerodynamic modeling fidelity was provided by Kim et al.,[14] who used Peters' three-state dynamic inflow model[15] to incorporate the effects of time lags in the development of the induced flow in response to the rotor aerodynamic loading. The yaw mode was suppressed in their fuselage dynamic, model, but blade aeroelastic effects were incorporated in fuller form than in previous works using elastic beam theory. Modeling of the interacting wake, using Burnham's[16] 1982 experimental data for a Boeing 747, followed a similar strategy to that adopted by Saito. The resultant model was used to refine the distinction between the behavior of helicopters with teetering, articulated, and hingeless rotors exposed by Saito's earlier work.

Using a simulation that also appears to have been of level 2, Curtiss and Zhou[2] generally supported Mantay's experimental conclusions regarding the loading induced on a helicopter during a vortex interaction, but pointed out that any pilot has a tendency to suppress, subconsciously, certain dynamics of the airframe. Their suggestion that a flight simulator be coupled to their code to study the pilot-induced damping of the helicopter's response underpins the recent resurgence of interest in the subject led by Padfield and Turner.[3,4] Their approach of assessing the helicopter's response to a vortex interaction in terms of the ADS-33 standard for rotorcraft handling qualities has potential as a practical method for evaluating the operational significance of wake encounters. Although their simulations have yet to proceed beyond level 2, these authors were the first to suggest[3] that neglecting the mutual interactions between the wake of the helicopter and the interacting aircraft (of the form that can be incorporated only in a level 0 aerodynamic simulation) might not be entirely appropriate under certain flight conditions.

Test Problem and Methodology

In the absence of experimental data against which to validate individual computations, we proceed by first selecting a simple model problem in which the physical effects of the frozen-vortex assumption can be clearly exposed. Starting from a highly simplified and constrained analytical model that implements the frozen-vortex assumption in its strongest possible form, a hierarchy of models is constructed in which elements of the assumption are incrementally relaxed. Analysis of the additional physical effects that emerge within the simulation at successive levels of the hierarchy will expose the effects of the frozen-vortex assumption, whereas an element of validation is provided by identifying those aspects of the predictions that remain consistent between successive levels of the hierarchy.

The highly simplified model system used to produce the results of this paper has just sufficient detail to allow the consequences of the frozen-vortex assumption to be investigated. The wake of the aircraft with which the helicopter is interacting is idealized as an isolated, infinite vortex with prescribed core structure. The helicopter itself is represented by an isolated, fully articulated rotor with flap, lag, and feather degrees of freedom. The hub of the rotor is not free to accelerate, and the rotor cyclic and collective controls are held fixed throughout the interaction. These rather drastic

simplifications prevent the fuselage rigid-body motions and other nonaerodynamic degrees of freedom in the real helicopter system from obscuring the effects of the aerodynamic interactions between the rotor, its own wake, and the interacting vortex that lie at the root of the frozen-vortex assumption. The subsequent effects of perturbations to the rotor loading and flapping on the fuselage dynamics, and any associated coupling, will be left largely to the reader's own inference.

Finally, to be at least partially representative of current practical concerns, attention will be focused on interactions with an idealized wake vortex that is aligned with the flight path of the helicopter and whose center passes through the rotor hub. (In later cases where the frozen-vortex condition has been eliminated, this geometry will be used as the starting condition for the interacting vortex.) Such a configuration of rotor and interacting vortex is sufficient to expose certain important implications of adopting the frozen-vortex assumption but by no means yields a comprehensive exploration of the full range of possible interaction scenarios. In particular, certain time-lag effects in the development of the flow near the rotor, which would become apparent if the helicopter were allowed to encounter a vortex lying transverse to its flight path, will not be excited very strongly in the calculations presented here.

If a series of rather restrictive assumptions are made, a set of simple analytic results can be derived for the thrust and flapping perturbations experienced by the rotor during this idealized vortex encounter. These results form the basis from which the more sophisticated and less constrained simulations presented in this paper can be evolved. Two basic results are required. The first result comes from standard linearized blade element theory,[17] which gives the thrust generated by a radial element on one of the rotor blades, located a fraction r of the rotor radius from the hub, as

$$\mathrm{d}C_T = (ca/2\pi)\left(\theta u_T^2 - u_T u_P\right)\mathrm{d}r \tag{1}$$

The velocity components (as a fraction of the rotor tip speed) respectively tangential and perpendicular to the rotor disc plane are, to first order in the blade flapping angle β and induced velocity normal to the rotor disc v_i,

$$u_T = r + \mu \sin\psi \tag{2}$$

and

$$u_P = v_i + \beta\mu\cos\psi + r\frac{\mathrm{d}\beta}{\mathrm{d}\psi} \tag{3}$$

The overall thrust generated on a single blade is then

$$C_T = \int_0^1 \frac{ca}{2\pi}\left(\theta u_T^2 - u_T u_P\right)\mathrm{d}r \tag{4}$$

The second result comes from a standard analysis of the response of an articulated, rotating blade to aerodynamic forcing.[17] The small-amplitude flapping dynamics of a rigid blade are described by

$$\frac{\mathrm{d}^2\beta}{\mathrm{d}\psi^2} + \omega^2\beta = \frac{1}{I_\beta}\int_0^1 r\,\mathrm{d}C_T \tag{5}$$

if the rotor hub is not free to accelerate.

To specialize these basic results to the idealized vortex enconter, the induced flow through the rotor is decomposed into a wake-induced component and vortex-induced component:

$$v_i = v_{\text{wake}} + v_{\text{vortex}}(r, \psi) \tag{6}$$

To obtain a tractable set of analytical expressions, v_{vortex} is held constant throughout the interaction, and v_{wake} is fixed in the distribution that it would have in the absence of the vortex. Together these restrictions force the analysis to represent the strongest possible (level 3) implementation of the frozen-vortex assumption.

With the controls held fixed, the blade feathering angle θ remains constant during the idealized vortex encounter. The sequence of operators

$$\int_0^{2\pi}\mathrm{d}\psi, \qquad \int_0^{2\pi}\sin^n\psi\,\mathrm{d}\psi$$

$$\int_0^{2\pi}\cos^n\psi\,\mathrm{d}\psi, \qquad n = 1, 2, \ldots$$

can then be applied in standard fashion to Eqs. (4) and (5) to transform them from their rotating blade frame of reference to a shaft-fixed frame of reference.[17] Subtracting the trimmed ($v_{\text{vortex}} = 0$) values from the results of this transformation gives the change in thrust and flapping of the rotor in response to the vortex-induced velocity field. The standard approach is to define the blade flapping in the shaft-fixed frame of reference in terms of a Fourier series in blade azimuth,

$$\beta = \beta_0 + \beta_{1s}\sin\psi + \beta_{1c}\cos\psi + \cdots \tag{7}$$

Following this approach, the vortex-induced perturbations to the rotor thrust and flapping predicted by this simple analysis are

$$\Delta C_T = (-\sigma a/2)\mu M^0_{1,0} \tag{8}$$

$$\Delta\beta_0 = (-\gamma_\beta/2)\mu M^1_{1,0} \tag{9}$$

$$\Delta\beta_{1s} = (4\gamma_\beta/3)[\mu^2/(\mu^2+2)]M^1_{1,0} \tag{10}$$

$$\Delta\beta_{1c} = [16/(2-\mu^2)]M^2_{1,0} \tag{11}$$

These results are strictly valid for an N-bladed rotor with negligible hinge offset ($\omega = 1$) having blades with zero twist and constant chord and aerofoil section along their span. In these expressions the disc-weighted moments of the vortex-induced velocity are

$$M^m_{n,p} = \frac{1}{2\pi}\int_0^{2\pi}\int_0^1 v_{\text{vortex}}(r, \psi)r^m\sin^n\psi\cos^p\psi\,\mathrm{d}r\,\mathrm{d}\psi \tag{12}$$

These integrals encapsulate the effect of both the stength and shape of the interacting vortex, as well as the orientation of the vortex with respect to the rotor, on the magnitude of the rotor's response. In the idealized vortex encounter v_{vortex} is antisymmetric with respect to the longitudinal axis of the rotor, and so $M^m_{n,p} = 0$ if n is even or $p \neq 0$.

Figure 1 shows a comparison, on the basis of these simple results, of the relative strengths of the vortex interactions that have been portrayed in previous studies of wake encounters. Points lying furthest away from the origin represent the strongest interactions, while the steeper the gradient of the line connecting the point to the origin, then the larger the thrust perturbation compared to the perturbation to the rotor disc tilt induced by the vortex. For comparison, estimates of the interaction severity for encounters of an assortment of helicopter types with the wakes trailed from large transport aircraft are also plotted. Interactions with the wakes trailed 2000 m behind Boeing 727, 747, and 767 aircraft at cruise speed have been estimated using the Lamb vortex model used by Saito[10,11] and Azuma et al.[12] The helicopters and aircraft are all assumed to be operating at maximum takeoff weight.

The liberal scatter of scenarios represented in previous studies is seen to encapsulate reasonably well the range of practically expected interactions. It is disappointing to note, though, that the single experimental point[7] on this figure appears to represent a very much weaker interaction than might be experienced by current helicopter types. This observation reinforces the pressing need for more relevant data for validation of simulations.

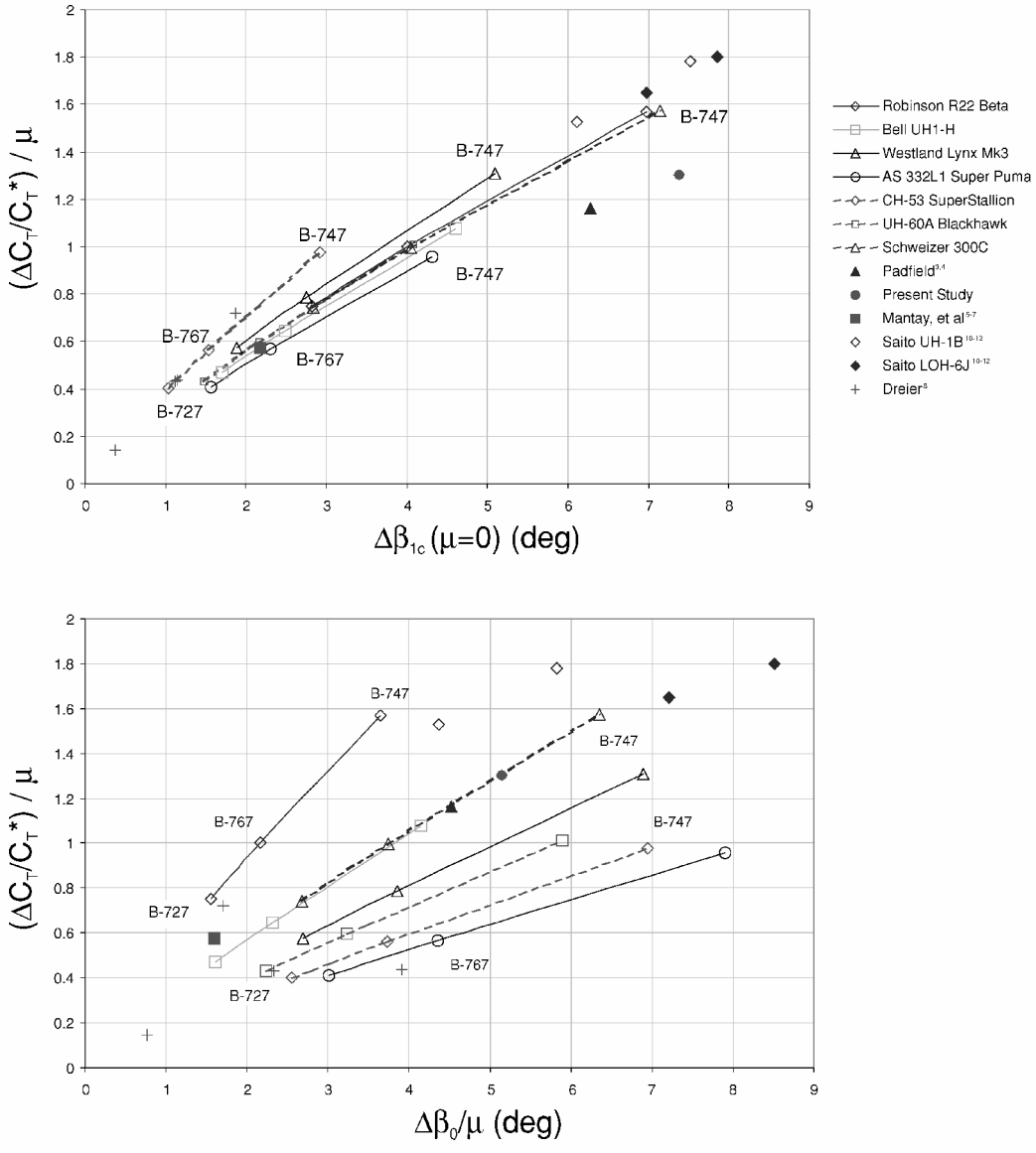

Fig. 1 Relative strengths of vortex interactions portrayed in previous studies.

Wake and Vortex Models

A physically more complete simulation of vortex interactions can be constructed as follows. If v is the velocity of the flow surrounding the rotor, then, in the absence of viscosity, the associated vorticity field $\omega = \nabla \times v$ evolves according to the unsteady vorticity transport equation,[18] which can be expressed in an inertial reference frame as

$$\frac{\partial}{\partial t}\omega + v \cdot \nabla\omega - \omega \cdot \nabla v = S \tag{13}$$

where S is the local source of vorticity. A simple transformation of this expression to a reference frame moving at the local flow velocity yields the better known Lagrangian free-vortex formalism.[19]

The vorticity transport model (VTM) described in the paper by Brown[18] is a direct computational fluid dynamics (CFD) type method for solving Eq. (13). Let $v(\omega)$ be the velocity field satisfying $\nabla \times v = \omega$. After casting the equations on a structured computational grid surrounding the rotor, Eq. (13) is marched through time using Toro's weighted average flux algorithm.[20] The velocity field $v = v(\omega)$ is found by inverting the differential form

$$\nabla^2 v = -\nabla \times \omega \tag{14}$$

of the Biot–Savart relationship using cyclic reduction[21] at the beginning of each time step. When used to model wake dynamics, the VTM is coupled into the rotor aerodynamic model by constructing the vorticity source S in terms of the shed and trailed vorticity from the blades of the rotors.

This approach yields very accurate predictions of rotor wake geometries[18] and forms a suitable basis from which to develop a hierarchy of simulations representing the various levels of implementation of the frozen-vortex assumption. A comparison of numerical results generated using the VTM with Harris' experimental data[22] for the flapping behavior of an isolated four-bladed rotor over a range of flight speeds is presented in Fig. 2. In this set of experiments, the rotor was trimmed to a preset thrust coefficient, the cyclic control angles were held fixed, and the free response of the rotor in flap was then measured. The error bars on the experimental data represent Harris' estimate of the resolution of his experiment. The good performance of the VTM is attributed to its ability to resolve accurately certain off-rotor flow features such as blade-vortex interactions and is indicative of its ability to capture properly the effects of forward speed on the self-induced distortion of the rotor wake. The model should thus be able to simulate wake-vortex interactions with comparable accuracy.

Hierarchy of Aerodynamic Models

The wake of the rotor can be represented as the vorticity distribution ω_W, arising from the aerodynamic loading on the rotor blades.

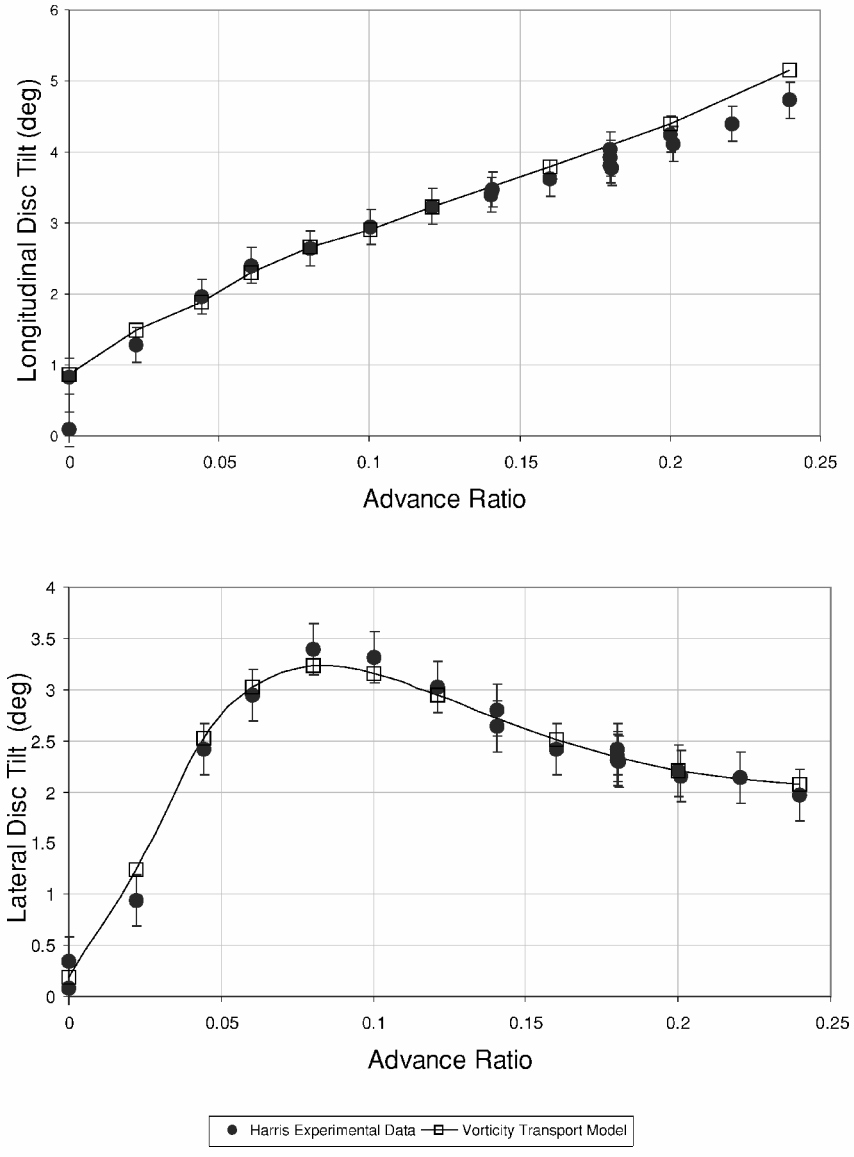

Fig. 2 Performance of the vorticity transport model in predicting rotor trim states.

Similarly, the interacting vortex can be represented as a vorticity distribution ω_V, subject to the initial condition that $\omega_V = \nabla \times v_{\text{vortex}}$. The linearity of Eq. (14) allows the problem of calculating the aerodynamics of the system [as governed by Eq. (13)] to be factored into a set of parallel problems, which can be delegated to the components A, W, and V of the aerodynamic model, providing that the velocity fields v_A, v_W, and v_V are suitably defined:

In A: solve,

$$S = S(v_A)$$

In W: solve,

$$\frac{\partial}{\partial t}\omega_W + v_W \cdot \nabla\omega_W - \omega_W \cdot \nabla v_W = S$$

In V: solve,

$$\frac{\partial}{\partial t}\omega_V + v_V \cdot \nabla\omega_V - \omega_V \cdot \nabla v_V = 0 \tag{15}$$

Using this approach, a hierarchy of simulations can be built from the VTM by interpreting the velocity fields v_A, v_W, and v_V in various ways to mimic the possible couplings between A, W, and V.

Equations (13) and (15) are completely equivalent if

$$v_A = -\mu + v(\omega_W) + v(\omega_V), \qquad v_W = -\mu + v(\omega_W) + v(\omega_V)$$
$$v_V = -\mu + v(\omega_W) + v(\omega_V) \tag{16}$$

The mutually induced distortion of the interacting vortex and helicopter wake and its effect on the rotor loading is fully accounted for using this approach, thus yielding a level 0 implementation of the frozen-vortex assumption.

A first level of approximation to the rotor aerodynamics results if v_V is re-defined so that

$$v_A = -\mu + v(\omega_W) + v(\omega_V), \qquad v_W = -\mu + v(\omega_W) + v(\omega_V)$$
$$v_V = -\mu \tag{17}$$

The dynamics of the interacting vortex are suppressed using this definition, resulting in a level 1 implementation of the frozen-vortex assumption.

Redefining v_W in addition so that

$$v_A = -\mu + v(\omega_W) + v(\omega_V), \qquad v_W = -\mu + v(\omega_W)$$
$$v_V = -\mu \tag{18}$$

decouples the evolution of the wake from any direct influence by the vortex-induced flowfield and yields a level 2 implementation of the frozen-vortex assumption.

Finally, a level 3 implementation of the frozen vortex condition results if v_A is redefined so that

$$v_A = -\mu + v(\omega_V), \qquad v_W = -\mu + v(\omega_W)$$
$$v_V = -\mu \tag{19}$$

In this situation the generation of rotor loads during the interaction is decoupled from any influences from the rotor wake.

Rotor Aerodynamic Model

All simulations presented in this paper use the same rotor aerodynamic model *A*. The helicopter is modeled as an isolated, counterclockwise-rotating rotor with three blades, a solidity of 0.05, and a Lock number of approximately 4.8. The blades are assumed to be rigid and to be connected to a fully articulated (but nonaccelerating) rotor hub with a collocated flap/lag hinge offset by 0.056 R. The aerodynamic loading on each blade is determined using a discrete implementation of unsteady lifting-line theory at a series of collocation points along the length of the blade. A variation of sectional lift coefficient with angle of attack given by the empirical correlation

$$C_L(\alpha) = \left[1 + 0.9325(1 + \cos\alpha)\, e^{-1108.8|\tan(\alpha/2)|^{4.9222}}\right] \sin 2\alpha \qquad (20)$$

is used throughout, giving a close match to published NACA 0012 data[23] in both attached and separated flow regimes.

In all cases the interacting vortex is (initially, in the case of level 0 simulations) aligned with the flight path of the helicopter and has the following radially symmetric velocity distribution.[8,9]

$$\frac{v_{\text{vortex}}}{v_c} = 1.359\,\frac{r}{r_c} \qquad \text{if} \qquad 0.0 \le \frac{r}{r_c} \le 0.60653$$

$$\frac{v_{\text{vortex}}}{v_c} = \frac{1 + \ln(r/r_c)}{r/r_c} \qquad \text{if} \qquad \frac{r}{r_c} > 0.60653 \qquad (21)$$

although it should be born in mind that this choice of core structure for the interacting vortex is essentially arbitrary. All results are presented for a vortex with $r_c = 0.4484$ and $v_c = 0.0857$, giving, from Eqs. (8–11), an expected thrust perturbation $\Delta C_T / C_T^* = 1.30\,\mu$ and flapping perturbations $\Delta\beta_0/\mu = 5.15$ deg and $\Delta\beta_{1c} = 7.38$ deg in hover. As shown in Fig. 1, this yields an interaction of comparable strength to those presented in previous numerical studies.

Results

The vortex-induced thrust and flapping response predicted by the hierarchy of VTM-based simulations and by the analytic results of Eqs (8–11) are compared in Figs. 3 and 4. Simulations of interactions with a vortex rotating in both positive [producing an upflow on the advancing side of the rotor and thus, from Eq. (8), an increase in the rotor thrust coefficient] and negative senses are presented for advance ratios between zero (hover) and 0.35. For each test case a set of rotor control angles is first obtained by trimming the rotor (in the absence of the vortex) to a thrust coefficient $C_T^* = 0.00449$ with zero cyclic flapping with respect to the hub axis. With the control angles locked at their trim settings, the rotor is then exposed to the vortex. After allowing sufficient time for the rotor to settle into its final state, its flapping and thrust response are measured. The coning response of the rotor has not been plotted; as for the rotor-vortex combination used in this study, its features are virtually identical to those of the thrust response of the rotor.

The results given in Eqs. (8–11) provide a very simple level 3 simulation of the idealized vortex interaction defined earlier. Compared to the linear blade aerodynamics assumed in the analytic approach, though, the VTM-based level 3 simulation has slight negative curvature in the attached flow regime [see Eq. (20)]. This is the cause of the vertical offset in the thrust perturbation predicted by the VTM-based simulation relative to the analytic results. Although the gradient of the predicted thrust response with advance ratio is very similar for both simulations, a slight softening of the gradient in the VTM-based simulation at high advance ratio, peculiar to interaction with a positive vortex, results from the progressive stalling of the most outboard part of the advancing side of the rotor. Poststall aerodynamics were neglected, of course, in deriving the analytic results.

Some small differences between the two simulations in the predictions of the rotor's longitudinal flapping are evident, but the strongest deviations occur in the vortex-induced perturbation to the lateral disc tilt. These deviations are largely caused by coupling between the rotor coning and the vortex-induced crossflow parallel to the disc plane—an effect that is present in the VTM-based model but that is not captured by the analytic model. Interestingly, convergence between the simulations is seen at high advance ratio, but extends only to interactions with a negatively rotating vortex where the associated coning perturbation acts to reduce this coupling.

Although level 3 simulation provides a very incomplete picture of the vortex interaction, this comparison yields a basic check on the validity of the blade aerodynamic model used throughout the remainder of this study. Building from this basis, the results of successively more comprehensive models for the vortex interaction will now be introduced. At each level of simulation, additional physical effects appear in the results. Some of these effects are undoubtedly spurious consequences of the modeling approach that has been adopted, but others are strongly indicative of real physics that has been neglected in the less representative physical models of the vortex interaction.

Advancing from level 3 to level 2 simulation introduces an extra degree of freedom in the blade aerodynamics by allowing the rotor inflow to vary in response to loading changes on the rotor. This extra degree of freedom prevents the drop-off in the thrust response at high advance ratio that is observed in the more constrained level 3 simulation. The most significant differences between the predictions of level 2 and level 3 simulations are confined to low advance ratio, however. The relatively large perturbations to the lateral tilt and the crossover in the thrust response between positive and negative vortex interactions can be traced to the same rather subtle variation with advance ratio of the inflow distribution over the rear half of the rotor disc that is responsible for the peak in the lateral tilt variation seen in Fig. 2. On the other hand, predictions of the rotor's longitudinal flapping response differ only weakly from the level 3 results, and this is most likely because the velocity field of the relatively strong interacting vortex used in this study dominates the wake's contribution to the lateral velocity gradient across the rotor.

The principal advance on level 2 simulation provided by level 1 and level 0 simulations is of course the ability of these models to capture the influence of the coupled dynamics of the interacting vortex and the rotor wake on the rotor's response to a vortex encounter. At high forward speed, where the wake-induced velocity is a less significant contibutor to the blade aerodynamic response than the freestream velocity, the results plotted in Fig. 4 suggest, however, that simulations having level 1 or level 0 complexity provide predictions of the rotor response to the vortex interaction which vary only slightly from the predictions of the simpler level 2 simulations.

This situation changes quite markedly at low forward speed, however. An interesting feature of the low-speed predictions of both the level 1 and level 0 simulations is that, unlike in level 2 and 3 simulation, the rotor does not settle to a steady state during the vortex encounter. In Fig. 5 the long-period variability (at frequencies lower than N per revolution) of the thrust and flapping response of the rotor is shown against advance ratio for the various types of simulation. At low forward speeds the variability in the thrust and flapping is comparable to, or even exceeds, the time-averaged response of the rotor (as plotted in Fig. 4). Most interestingly, the level 1 simulation predicts unsteadiness in the vortex-induced rotor response to persist for all advance ratios below about 0.10, whereas the level 0 simulation predicts unsteadiness to exist only over an intermediate band of advance ratios from about 0.02 to 0.10.

Figure 6 compares the changes in the morphology of the rotor wake and the interacting vortex that the VTM-based level 1 and level 0 simulations predict to accompany a vortex encounter. The wake and interacting vortex are represented as surfaces on which the vorticity in the flow has constant magnitude. A relatively low vorticity contour has purposely been selected in these plots to capture the global geometry of the helicopter wake while suppressing the finer details embedded within the wake structure. Predictions at two different forward speeds are shown: the plots at right illustrate the wake morphology at an advance ratio of 0.35, where the wake of the unperturbed rotor (as shown in the upper plot) is dominated by a pair of aeroplane-like, counter-rotating wing-tip vortices. The plots at left show the predicted wake morphology at an advance ratio of

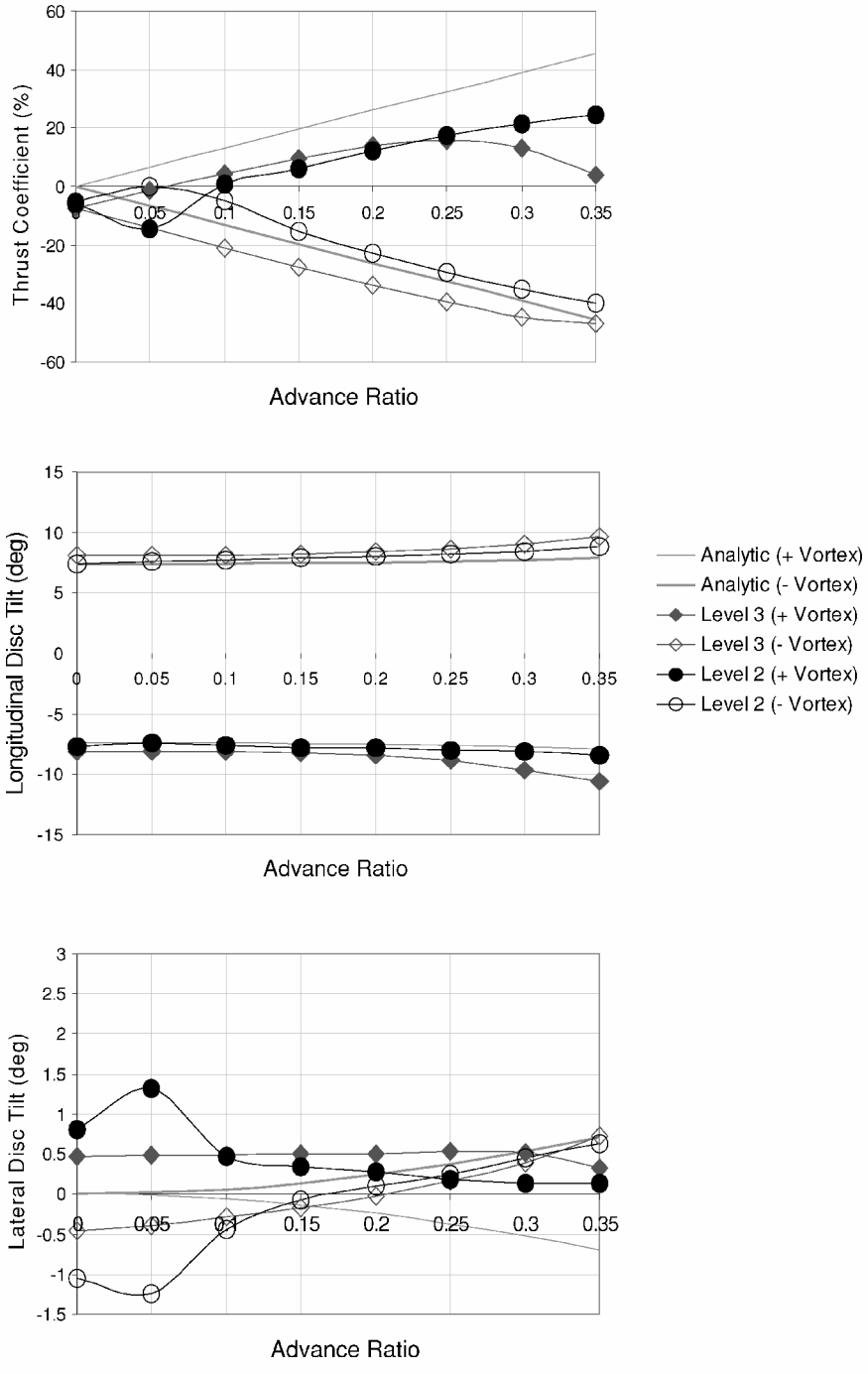

Fig. 3 Perturbations to rotor trim states in response to a vortex interaction (level 2 and 3 simulations).

0.05, where the wake of the unperturbed rotor is in an intermediate state between its high-speed aeroplane-like structure and the tubular form found at lower advance ratios.

The middle and lower plots of Fig. 6 show, as expected, the wake-vortex morphology predicted by the level 1 and level 0 simulations to be very similar at the higher advance ratio. As the advance ratio of the rotor is reduced, the level 1 simulation shows the rotor wake to become increasingly distorted by the presence of the vortex, until, at advance ratios less than about 0.1, parts of the wake are sporadically reingested through the rotor disc. Figure 6b shows this process about to occur during a level 1 simulation of the vortex interaction at $\mu = 0.05$. The thrust and flapping fluctuations result from the rotor loading changes that accompany this unsteadiness in the rotor flowfield.

If, though, the interacting vortex is allowed to convect freely under the action of the ambient velocity field as in the level 0 simulations, then as the advance ratio of the rotor is reduced the same effect is observed only up to a point. The mutually induced distortion of the rotor wake and interacting vortex increasingly results in the vortex being displaced as it passes close to the rotor (Fig. 6c). At advance ratios lower than about 0.02, the interacting vortex is displaced so far from the rotor plane that any unsteadiness in the fluid-dynamic interaction between the rotor wake and interacting vortex has only a weak effect on the dynamics of the rotor.

The strong effects of the rotor wake-induced displacement of the interacting vortex at low forward speed are most clearly apparent in the results for the mean response of the rotor. Comparison of the thrust and flapping perturbations predicted by the level 1 and level 0 simulations shows that the response of the rotor predicted by the level 1 simulation at low advance ratios is largely a spurious consequence of overconstraining the interacting vortex. If the interacting vortex is allowed to convect freely, then the predicted magnitude

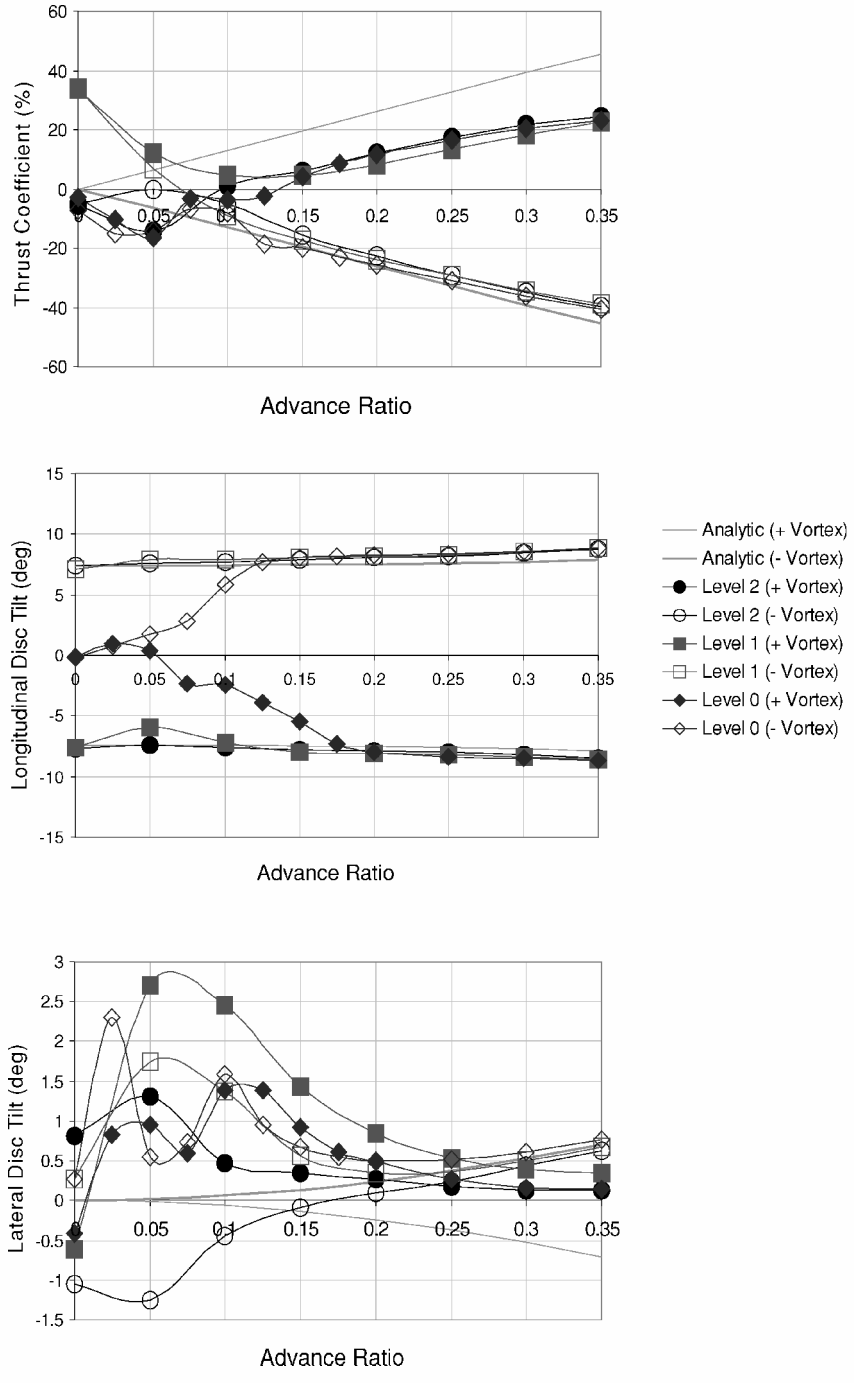

Fig. 4 Perturbations to rotor trim states in response to a vortex interaction (level 0 and 1 simulations).

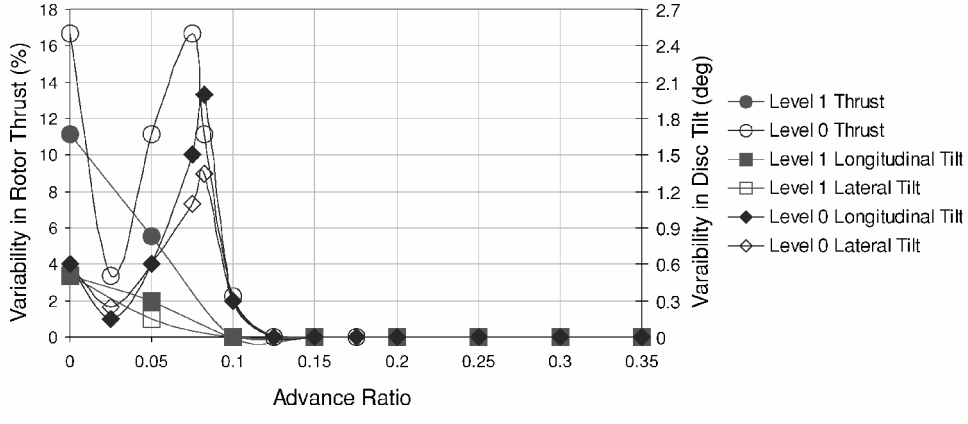

Fig. 5 Variability in rotor thrust and flapping (level 0 and 1 simulations).

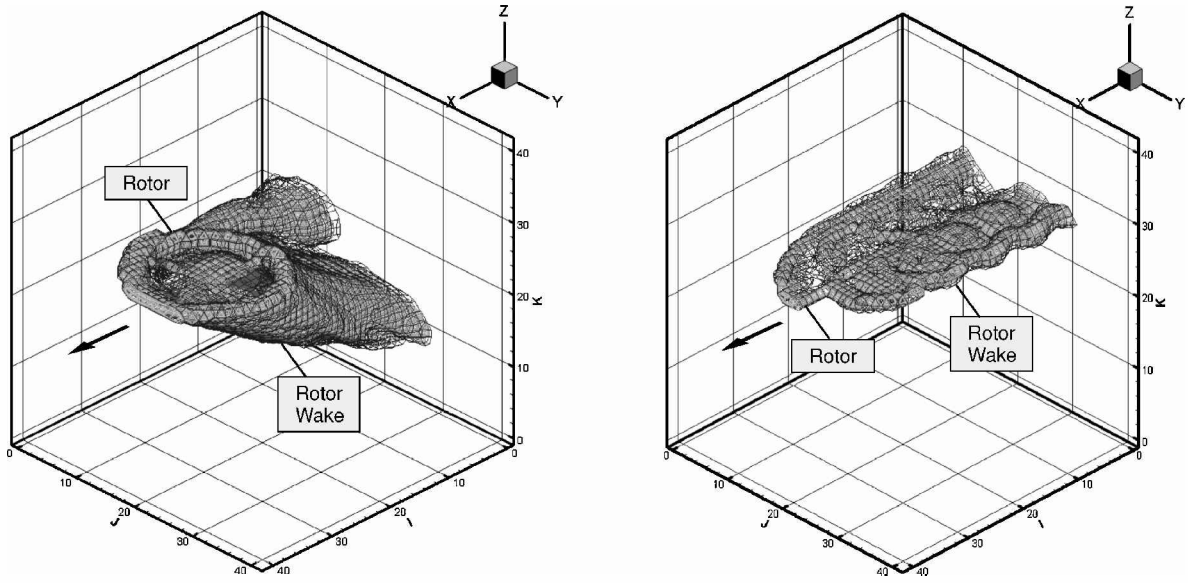

a) In trimmed flight

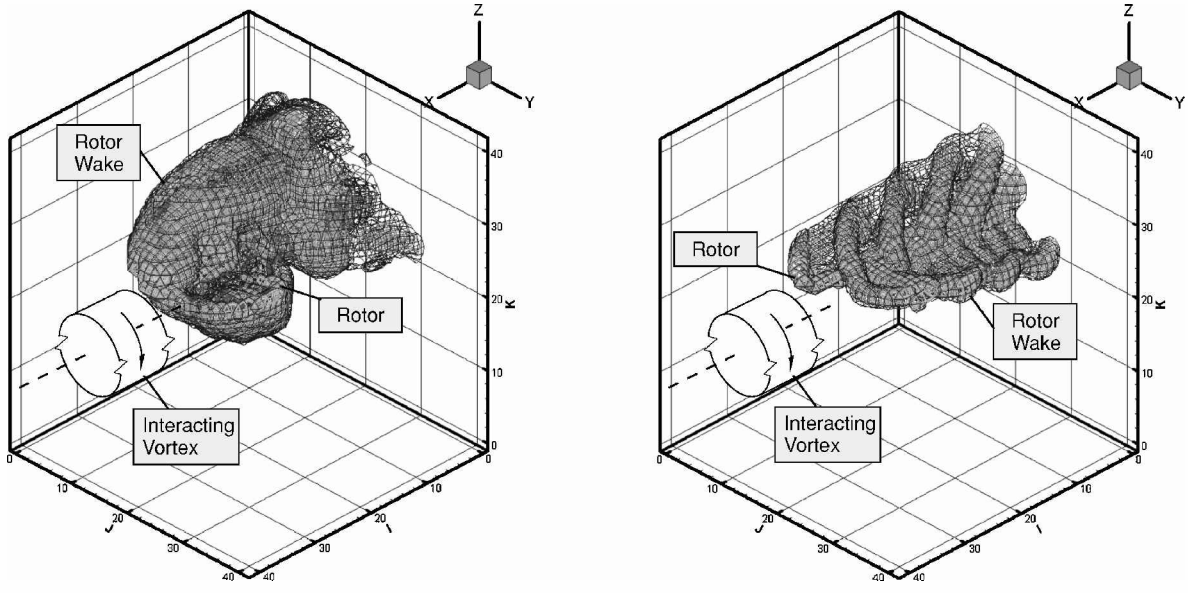

b) Level 1 simulation

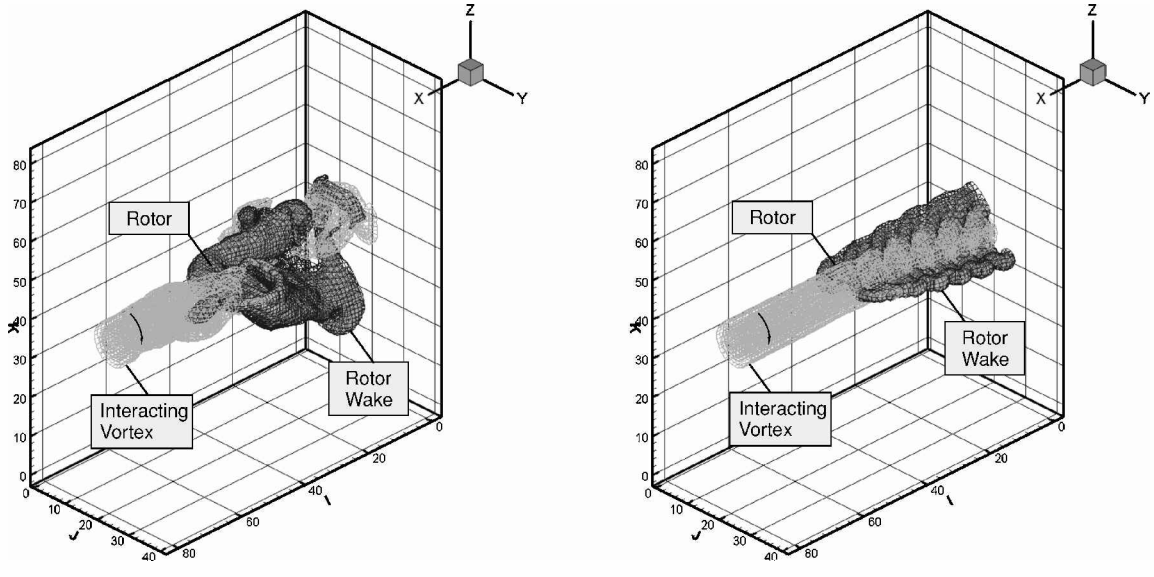

c) Level 0 simulation

Fig. 6 Wake morphology at $\mu = 0.05$ (left) and $\mu = 0.35$ (right) (positive vortex).

of the rotor thrust and flapping response, at low forward speeds, is significantly reduced in comparison.

Conclusions

The principal aim of this paper has been to provide a systematic and hierarchical assessment of the validity of the so-called "frozen vortex assumption." This assumption has traditionally been invoked to allow the mutually induced distortion of the helicopter's wake and the wake of the interacting aircraft to be neglected during numerical simulations of a helicopter's dynamic response to a vortex encounter.

The results presented in this paper suggest that a relatively simplistic approach to the modeling of the wake and vortex dynamics (embodying the frozen-vortex assumption in its stronger forms) might indeed be adequate for describing the rotor response to a vortex encounter at high forward speed. At the low forward speeds most relevant to operations near airports, however, oversimplified modeling of the mutually induced distortion of the rotor wake and the interacting vorticity field is shown to significantly overpredict the mean loading and flapping response of the rotor.

If taken at face value, these results suggest that vortex encounters under terminal flight conditions might not pose as significant a hazard to operations as has been thought. The interesting possibility also suggests itself that rotorcraft might possess an obvious practical advantage over fixed-wing aircraft by being able to ameliorate the severity of their encounters with aircraft wakes merely by constraining their forward speed while traversing a volume of space (for example, an airfield's terminal control area), which is known to be contaminated by the presence of aircraft trailing vortices.

This might however, be an overly simplistic interpretation of the results presented here. Low-speed interactions appear to be characterized by strong fluctuations in the rotor response. These fluctuations have implications for the handling qualities of the helicopter, especially under terminal flight conditions, that can outweigh the beneficial effects of any reduction in the mean loading and flapping response of the rotor obtained by flying at reduced speed.

The results of this paper suggest that the physics of wake interactions is somewhat more complicated than has been portrayed in previous numerical studies of the problem. They also suggest that extrapolation of the results of previous studies, especially to low-speed flight conditions, might not be entirely appropriate. Nevertheless, the results presented here have been obtained in the context of a single, relatively simple (but hopefully somewhat indicative) interaction scenario. This work thus serves primarily to emphasize the need for a more complete study (backed up by experimental validation) of vortex interactions, under flight conditions that are specifically relevant to terminal flight operations, before any firm conclusions regarding the hazards posed by wake encounters during low-speed terminal flight conditions can be reached.

Acknowledgments

The work described in this paper is supported by the ongoing U. K. Engineering and Physical Sciences Research Council Grant GR/L/013136 "Helicopter Response to Vortex Encounters in the Near-Airfield Environment" and an Overseas Research Student Award.

References

[1]"The Potential of Rotorcraft to Increase Airport Capacity," Royal Aeronautical Society Conference, London, Oct. 1999.

[2]Curtiss, H. C., and Zhou, Z. G., "The Dynamic Response of Helicopters to Fixed Wing Aircraft Wake Encounters," *International Wake Vortex Symposium*, Washington, DC, 1991.

[3]Padfield, G. D., and Turner, G. P., "Helicopter Encounters with Aircraft Vortex Wakes," *25th European Rotorcraft Forum*, Rome, 1999.

[4]Padfield, G. D., and Turner, G. P., "Helicopter Encounters with Aircraft Vortex Wakes," *The Aeronautical Journal*, Vol. 105, No. 1043, 2001, pp. 1–8.

[5]Dunham, E. R., Holbrook, G. T., Mantay, W. R., Campbell, R. L., and van Gunst, R. W., "Flight Test Experience of a Helicopter Encountering an Airplane's Trailing Vortex," *32nd Annual National V/STOL Forum of the American Helicopter Society*, AIAA-Paper 1063, Washington, DC, May 1976.

[6]Mantay, W. R., Holbrook, G. T., Campbell, R. L., and Tamaine, R. L., "Flight Investigation of the Response of a Helicopter to the Trailing Vortex of a Fixed Wing Aircraft," *AIAA 3rd Atmospheric Flight Mechanics Conference*, AIAA, New York, June 1976.

[7]Mantay, W. R., Holbrook, G. T., Campbell, R. L., and Tamaine, R. L., "Helicopter Response of an Airplane's Trailing Vortex," *Journal of Aircraft*, Vol. 14, No. 4, March 1977, pp. 357–363.

[8]Dreier, M. E., "The Influence of a Trailing Tip Vortex on a Thrusting Rotor," M.S. Thesis, Dept. of Aerospace Engineering, Pennsylvania State Univ., State College, March 1977.

[9]McCormick, B. W., Tangler, J. L., and Sherrieb, H. E., "Structure of Trailing Vortices," *Journal of Aircraft*, Vol. 5, No. 3, Sept. 1968, pp. 260–267.

[10]Saito, S., Azuma, A., Kawachi, K., and Okuno, Y., "Study of the Dynamic Response of Helicopters to a Large Airplane Wake," *12th European Rotorcraft Forum*, AIAA-Paper-42, Garmisch-Partenkirchen, 1986.

[11]Saito, S., Azuma, A., Kawachi, K., Okuno, Y., and Hasegawa, T., "Numerical Simulations of Dynamic Response of Fixed and Rotary Wing Aircraft to a Large Airplane Wake," *13th European Rotorcraft Forum*, AIAA-Paper-7, Arles, Sept. 1987.

[12]Azuma, A., Saito, S., and Kawachi, K., "Response of a Helicopter Penetrating the Tip Vortices of a Large Airplane," *Vertica*, Vol. 11, No. 1, 1987, pp. 65–76.

[13]Azuma, A., and Kawachi, K., "Local Momentum Theory and Its Application to the Rotary Wing," *Journal of Aircraft*, Vol. 16, No. 2, 1979, pp. 6–14.

[14]Kim, K. C. Bir, S. G., and Chopra, I., "Helicopter Response to an Airplane's Vortex Wake," *12th European Rotorcraft Forum*, AIAA-Paper-43, Garmisch-Partenkirchen, Sept. 1986.

[15]Gaonkar, G. H., and Peters, D. A., "Review of Dynamic Inflow Modeling for Rotorcraft Flight Dynamics," *Vertica*, Vol. 12, No. 3, 1988, pp. 213–242.

[16]Burnham, D. C., "B-747 Vortex Alleviation Flight Tests: Ground Based Sensor Measurements," U.S. Department of Transportation/Federal Aviation Administration, Rept. DOT-FAA-RD-81-99, Washington, DC, Jan. 1982.

[17]Johnson, W., *Helicopter Theory*, Princeton Univ. Press, Princeton, NJ, 1980, Chap. 5.

[18]Brown, R. E., "Rotor Wake Modeling for Flight Dynamic Simulation of Helicopters," *AIAA Journal*, Vol. 38, No. 1, 2000, pp. 57–63.

[19]Leishman, J. G., *Principles of Helicopter Aerodynamics*, Cambridge Univ. Press, New York, 2000, p. 496, Chap. 10.

[20]Toro, E. F., "A Weighted Average Flux Method for Hyperbolic Conservation Laws," *Proceedings of the Royal Society of London, Series A: Mathematical and Physical Sciences*, Vol. 423, No. 1864, 1989, pp. 401–418.

[21]Schumann, U., and Sweet, R. A., "A Direct Method for the Solution of Poisson's Equation with Neumann Boundary Conditions on a Staggered Grid of Arbitrary Size," *Journal of Computational Physics*, Vol. 20, No. 2, 1976, pp. 171–182.

[22]Harris, F. D., "Articulated Rotor Blade Flapping Motion at Low Advance Ratio," *Journal of the American Helicopter Society*, Vol. 17, No. 1, 1972, pp. 41–48.

[23]Prouty, R. W., *Helicopter Performance, Stability, and Control*, 2nd ed., Krieger, Malabar, FL, 1995, p. 731, Chap. 6.